

DETERMINATION OF PROPAGATION MECHANISMS USING WIDEBAND MEASUREMENT TECHNIQUES

H.-J. Li, H.-C. Lin, C.-C. Chen, T.-Y. Liu, and Z.-Y. Lane

Department of Electrical Engineering
National Taiwan University
Taipei, Taiwan, R.O.C.

- 1. Introduction**
 - 2. Basic Wideband Measurement Principle**
 - 3. Measurement Procedure**
 - 4. Wideband Measurements for Different Propagation Mechanisms**
 - A. Measurement of Direct Wave
 - B. Measurement of Reflection Coefficients
 - C. Measurement of Edge Diffraction
 - D. Measurement of Radar Cross Section (RCS)
 - 5. Experimental Results**
 - 6. Conclusion**
- References**

1. INTRODUCTION

The mechanisms behind electromagnetic wave propagation can generally be attributed to direct wave, reflection, diffraction, and scattering. In outdoor environments all scatterers such as buildings, vehicles, pedestrians, light poles, trees, curbs and ground, etc, will contribute to the total received field. The measurements of the channel characteristics can be divided into narrowband measurements and wideband measurements. Narrowband measurements can only measure the power level, but contributions from different paths cannot be differentiated. Wideband measurements can measure delay profiles, which provide information of the amplitude and time delay of each

path wave. Wideband measurement systems can be classified as the direct *RF* pulse system, the spread spectrum sliding correlator system [1], and the swept frequency network analyzer system [2, 3]. The direct *RF* pulse system has a low sensitivity and a low dynamic range, and is only useful for short-range measurements. The sliding correlator system is commonly used to measure cellular channel characteristics [1]. Its resolution is limited by the chip duration. The vector network analyzer system can have a very wide bandwidth. However, this system requires that both transmitting and receiving antennas be simultaneously cable-connected to the network analyzer and this limits its applications in indoor environments or in short distance areas. Because the network analyzer system has a very wide bandwidth and therefore can give a very fine range or time delay resolution, it is a powerful tool for analyzing the wave propagation mechanisms.

In the literature, the reflection coefficients or diffraction coefficients are usually derived from the continuous wave (CW) measurements. However, it is very difficult to isolate each single propagation mechanism because the measured field is the superposition of all path waves. Therefore the results obtained by CW measurements can be incorrect. Using the sliding correlator system to determine reflection coefficients of rough surface has been reported [4]. In this paper we will use the network analyzer system to measure the delay profiles and to determine the reflection and diffraction coefficients by isolating each path. In Section 2 basic wideband measurement principle will be briefly discussed. The measurement procedure will be described in Section 3. In Section 4 the wideband measurements for different propagation mechanisms will be proposed. The comparison between the measured and simulated results will be demonstrated in Section 5. Discussions and conclusions will be given in Section 4.

2. BASIC WIDEBAND MEASUREMENT PRINCIPLE

The impulse response of a radio channel can be expressed by

$$H(t) = \sum a_i \delta(t - \tau_i), \quad (1)$$

where a_i and τ_i represents the amplitude and the time delay of the i^{th} path wave respectively. If the transmitted signal is a CW wave with radial frequency ω , the received field can be expressed as

$$E(k) = \sum a_i e^{jk \tau_i}, \quad (2)$$

where $k = \omega/c$, $r_i = c\tau_i$ with c denoting the speed of light and r_i denoting the total path length of the i^{th} path.

We can use wideband measurement to determine a_i and τ_i (or r_i). The complex frequency responses (both amplitude and phase) are first measured and then the inverse fast Fourier transform (IFFT) is applied to obtain the delay profile. The peak values and the corresponding positions represent the magnitudes and time delays (or path lengths) of the multipath components. However, whether each path wave can be accurately resolved depends on the delay time difference of the delay, the bandwidth available, and the sampling interval used in the measurement. The wider the bandwidth is, the finer the resolution is. However, the allowable bandwidth is limited by the measurement system, such as the antenna bandwidth. Furthermore, the peak values obtained by using IFFT may not represent the true peaks. Thus the reflection coefficient or edge diffraction coefficient derived from these peaks can be incorrect. To obtain accurate measurement of a_i and τ_i the following factors will be carefully considered in wideband measurements and signal processing.

1. Bandwidth and the number of frequency points being sampled. Denote the bandwidth as BW and the number of frequency points as I, then the frequency increment is $\Delta f = \text{BW}/(I - 1)$. After applying IFFT on the frequency responses, the range of time delay in the delay profile is $(0, 1/\Delta f)$ and the time resolution is $1/\text{BW}$. Therefore in selecting I , one should consider the possible longest time delay. If I is not large enough, or if Δf is not small enough, the time delay obtained may be ambiguous. The bandwidth required depends on the difference of the time delay or the difference in path length of multipaths. In microcell or indoor environments the path length difference is smaller, a wider bandwidth should be used in order to resolve different path waves.

2. Zero padding. In discrete Fourier transforms, what we obtained are discrete sampled values. If the delay profile changes too fast, the sampled peak may not be the true peak. If we use the sampled peak to represent a_i , then the derived result may be inaccurate. To avoid this, zeros can be padded in the frequency domain data before applying IFFT. Because Zero padding is equivalent to an interpolation process, the more zeros are padded, the finer the sampled interval will be in the delay profile, and it is more likely that the true peak can be sampled.

3. Window function. The window function applied in the FFT will affect the sidelobe level. Sidelobes may cause misjudgment of multipath. To avoid the misjudgment, we can use those window functions with smaller sidelobe level, such as the Hamming window. However, the application of Hamming window will degrade the range resolution.

3. MEASUREMENT PROCEDURE

The quantities to be measured are the frequency response of the radio channel. However, the characteristics of all components used in the measurement systems, such as amplifiers, cables, antennas, etc., are also functions of frequency. Therefore, the effect of frequency response of the measurement system should be eliminated. The elimination procedure can be proceeded as follows:

1. Place the receiving antenna in front of the transmitting antenna at a distance of 1 meter and at the same height. Record the frequency response and denote it as $E(k, r_o)$. Note that this measurement should be conducted in an open environment or in an anechoic chamber so that multipath effect is minimized.

2. At each test position, record the frequency response and denote it as $E(k, r)$.

3. Divide $E(k, r)$ by $E(k, r_o)$ and denote it as

$$\tilde{E}(k, r) = E(k, r)/E(k, r_o). \quad (3)$$

With this procedure the effect of the frequency response of the measurement system can be eliminated. It is noted that, the quantity $\tilde{E}(k, r)$ defined in (3) represents the propagation loss relative to that obtained at the reference distance (1m). If we apply IFFT on $\tilde{E}(k, r)$ to obtain the delay profile, the abscissa in the delay profile represents the excess delay time or excess traveling distance with respect to the reference location.

However, the ordinate value should be carefully defined. It is noted that the number of zeros padded and the window function used will affect the amplitude of the resultant Fourier transforms. To make the ordinate value representing the propagation loss at certain traveling distance relative to the direct path loss at the reference separation, the following calibration procedure is proposed.

1. Determine the number of frequency points to be measured (N), the number of zeros to be padded (M), and the window type to be applied. The sum of N and M should be powers of 2.

2. Multiply an array $\{\mathbf{b}_1, \dots, \mathbf{b}_N\}$ with the desired window function, where $\mathbf{b}_1 = \mathbf{b}_2 = \dots = 1$, pad M zeros, and then take the IFFT. There will be a peak at the origin. Denote the peak value as P_o (in dB), which represents the amplitude after IFFT of the direct wave with a reference separation.

3. Multiply $\tilde{E}(k, r)$ with the same window function, pad M zeros, and take the IFFT. The delay profile value (in dB scale) is then subtracted by P_o . The resultant ordinate value will represent the propagation loss at each excess traveling distance relative to the direct path loss with a reference separation.

4. WIDEBAND MEASUREMENTS FOR DIFFERENT PROPAGATION MECHANISMS.

There are four types of propagation mechanisms, namely the direct wave, reflection, diffraction and scattering. In this section we will briefly describe the properties of these propagation mechanisms and propose using wideband measurement techniques to measure these properties.

A. Measurement of Direct Wave

Consider two antennas with gains G_t and G_r and at a separation of d . Under the far field condition, the propagation loss of the direct wave, defined as the ratio of the received power P_d to the transmitted power P_t , can be expressed by

$$P_d/P_t = \frac{G_t G_r \lambda^2}{(4\pi d)^2}, \quad (4)$$

The propagation loss is inversely proportional to the square of distance.

Through the calibration procedure as described in the previous section, the first peak in the delay profile represents contribution from the direct path. The relative propagation loss is equal to $(d_o/d)^2$, where d_o is the reference distance.

B. Measurement of Reflection Coefficients

As shown in Fig. 1, two directive antennas are pointing to the reflecting point of the wall and the incident angle is Θ_i . Let the distances from the reflecting point to the transmitting antenna and the receiving antenna be d_1 and d_2 respectively and the separation between the

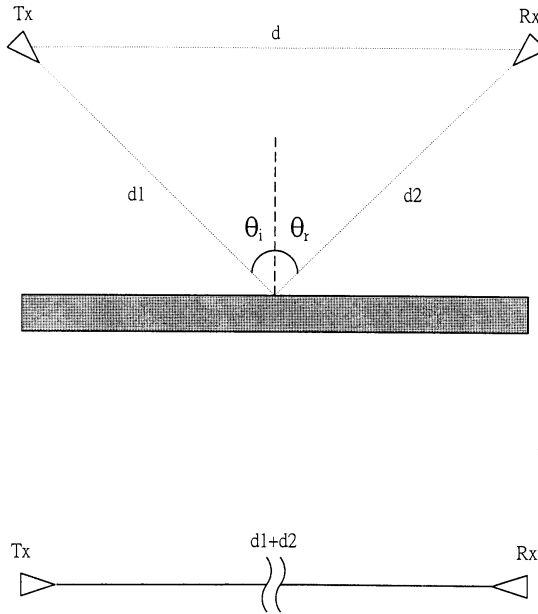


Figure 1. Geometry of wall reflection measurement.

two antennas be d . In the delay profile, there are peaks positioned at distances d and $d_1 + d_2$. Denote the value of the wall-reflected component as A_r . To determine the wall reflection coefficient, we then place the two antennas at a separation of $d_1 + d_2$ and point to each other. Repeat the delay profile measurement and denote the amplitude of the first peak as A_d . The wall reflection coefficient is then equal to $\Gamma = A_r/A_d$.

If the wall surface is a rough surface, the same technique can be applied to obtain the effective reflection coefficients. It is noted that the reflection coefficient of a rough surface is a function of frequency. Therefore, the reflection coefficient derived from wideband measurements can be considered as the mean value averaged over the frequency band. To verify the effectiveness of this proposed method, we can change the antenna position but keep the incident angle constant, and then repeat the measurement and compare the results.

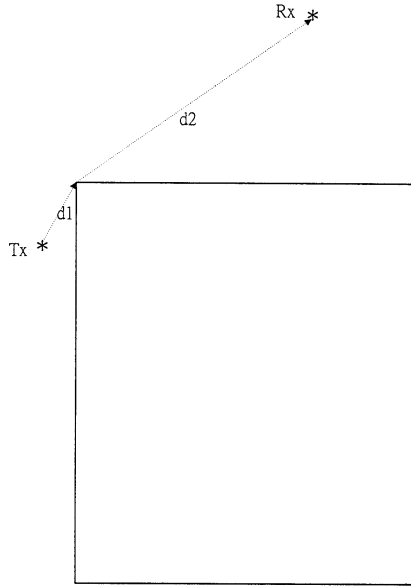


Figure 2. Geometry of edge diffraction measurement.

C. Measurement of Edge Diffraction

Edge diffraction coefficient is a function of the dielectric constant, the extended angle of the wedge, the incident angle, the diffraction angle, the frequency and the polarization. The formulation for diffraction coefficients can be found in [5]. The diffraction coefficient of a wall edge can be calculated by substituting the corresponding parameters into those equations. As shown in Fig. 2 the distances between the wall edge to the transmitting antenna and receiving antenna are d_1 and d_2 respectively. The diffracted power P_D can be expressed by

$$P_D = \frac{|D|^2 \cdot G_t G_r}{d_1 d_2 (d_1 + d_2)} \cdot P_t. \tag{5}$$

With wideband measurements, contribution from the edge diffraction can be derived from the amplitude of the peak, located at a delay length of $d_1 + d_2$. Denote the peak value as D_1 . The two antennas are then separated at a distance of $d_1 + d_2$ and pointed to each other. Denote the direct path contribution as D' . The wall diffraction coefficient can be derived from the ratio D_1/D' . By changing the positions of the

transmitting and/or receiving antenna, the edge diffraction coefficients for different incident angles and diffraction angles can be obtained.

D. Measurement of Radar Cross Section (RCS)

The RCS of a scatterer highly depends on the frequency, the polarization, and the observation direction. Denote the RCS of a scatterer as σ , the distances of the scatterer to the transmitting and receiving antennas as d_1 , and d_2 , and the antenna's gains as G_t and G_r respectively. The received scattered power can be expressed by

$$P_r = \frac{P_t \cdot G_t}{4\pi d_1^2} \cdot \sigma \cdot \frac{G_r \cdot \lambda^2}{(4\pi d_2)^2}. \quad (6)$$

When the two antennas are pointed to each other and separated by a distance of $d_1 + d_2$, the received power is

$$P_d = \frac{P_t \cdot G_t \cdot G_r \cdot \lambda^2}{[4\pi(d_1 + d_2)]^2}. \quad (7)$$

Dividing P_r by P_d , we have

$$P_r/P_d = \frac{\sigma(d_1 + d_2)^2}{4\pi d_1^2 d_2^2}, \quad (8)$$

$$\sigma = \frac{4\pi d_1^2 d_2^2}{(d_1 + d_2)^2} \left(\frac{P_r}{P_d} \right). \quad (9)$$

In the delay profiles we can find the corresponding peaks and substituting them into Eq. (9) to determine the RCS of the scatterer. Because the RCS is highly dependent on the operating frequency, especially when the object shape is complex and the dimension is large compared with a wavelength, the RCS so obtained is the value averaged over the frequency band.

E. Delay profile of a radio channel

A real radio channel is usually complicated and contains different propagation mechanisms. The measured delay profile can provide information of the amplitude and delay length of multipath waves. However, it is very difficult to identify each path wave except those path

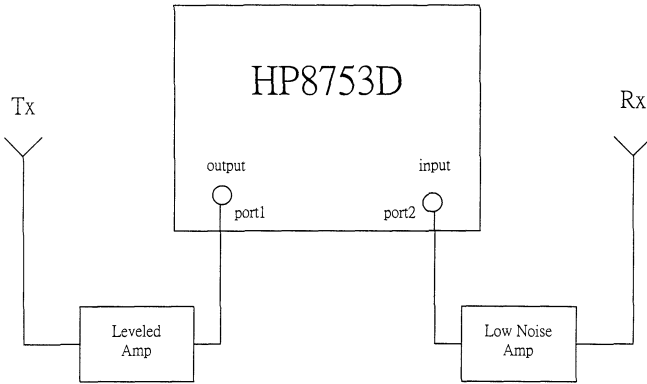


Figure 3. Block diagram of the measurement system.

components such as the direct path, single reflection due to ground or wall, single edge diffraction and reflection from big building. Nevertheless, information such as attenuation and delay time of multiple paths, root mean square delay spread, and the local average power etc, can be derived from wideband measurements or delay profiles.

5. EXPERIMENTAL RESULTS

In this section, some experimental results are provided to demonstrate the effectiveness of our proposed method.

The block diagram of the measurement system is shown in Fig. 3. The transmitting and receiving antennas are both vertically polarized $\lambda/2$ dipole antennas. The frequency is swept from 2.2 ~ 2.6 GHz and the number of frequency points is 401. As described in the previous section, the two antennas are first separated by 1 meter apart and placed at the same height of 3 meters. The frequency responses are stored and denoted by $E(k, r_o)$. Then the receiving antenna is moved along a straight line and is kept at a constant height of 3m. The frequency responses at a separation r are denoted by $E(k, r)$. $E(k, r)$ are then divided by $E(k, r_o)$ to give the relative propagation loss response $\tilde{E}(k, r)$. To obtain the delay profile, $\tilde{E}(k, r)$ is padded with zeros to a total number of 1024 frequency points and the Hamming window function is applied in the IFFT.

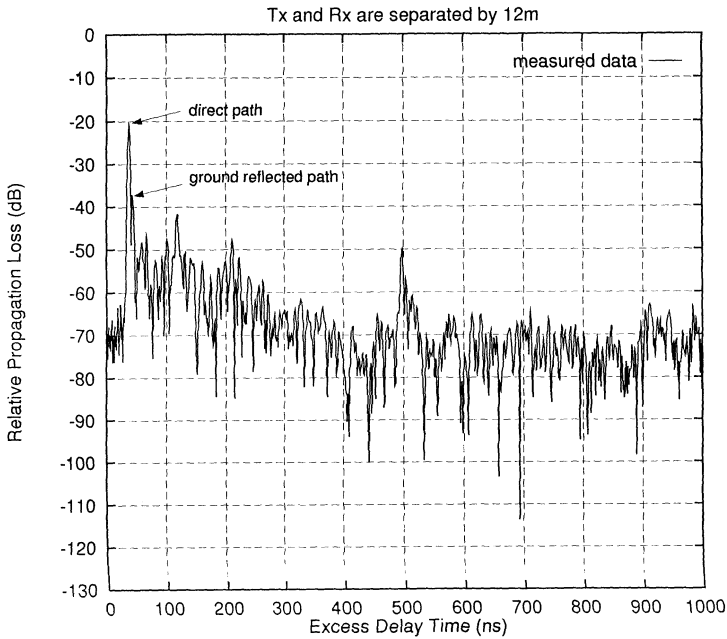


Figure 4. The delay profile measured at a separation of 12m.

Fig. 4 shows the delay profile measured at a separation of 12m. From the delay profile we can identify the peaks corresponding to the direct path and the ground reflection. We plot the delay profile for each location and from the plot we can find the peak corresponding to the direct wave. The plot of the relative propagation loss of the direct wave versus distance is shown in Fig. 5. The theoretical free space loss versus distance is also shown in the figure by the dashed curve. The deviation between the measured and the theoretical values is within 1dB.

Next the reflection coefficient of a brick wall with small roughness is to be determined. Two vertically polarized log-periodic antennas are pointed to the reflection point of the wall as shown in Fig. 1. For each incident angle, the distances d_1 and d_2 and the frequency responses covering the range from 2GHz to 3GHz are recorded. With this bandwidth the reflected path and the direct path can be easily resolved, and the reflection coefficient can be determined by the procedure as described in the previous section. The derived reflection coefficients for various incident angles are shown in Fig. 6. Assuming that the

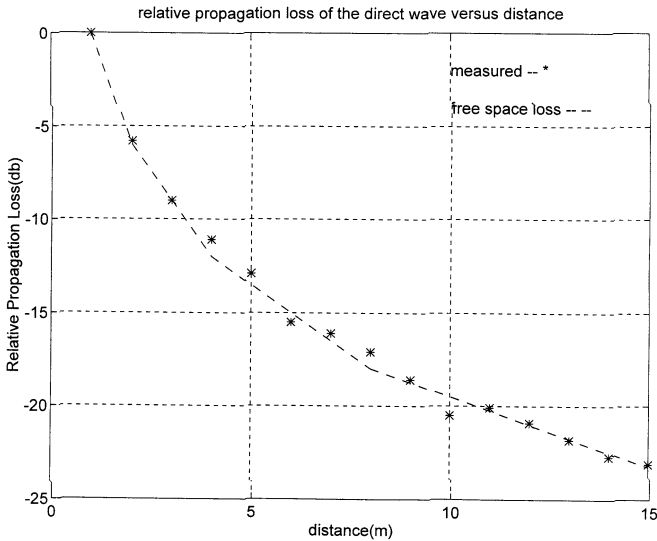


Figure 5. Plot of the relative propagation loss of the direct wave versus distance.

wall is an ideal smooth surface and its dielectric is $\epsilon_r = 6 - j$, the calculated reflection coefficients are shown in Fig. 6 for comparison. As the incident angle is increased, it is more difficult to differentiate the direct path and the reflected path and the deviation between the measured and the calculated values becomes greater.

To measure the diffraction coefficient we select a corner part of the building. The measurement environment is sketched in Fig. 7. The receiving antenna is moved along a straight line parallel to the wall surface and measurement is repeated every 1.2m. There is a line of sight for the first four positions. After that the direct path is obstructed. From the 5th position to the 14th position there is a single diffracted wave. After the 14th position the wave diffracted by the first corner edge is obstructed by the second corner.

For each position we obtain the delay profile and from the successive delay profiles we can identify the peak due to either the direct path or the diffracted path. With the geometry of Fig. 7 we can also apply the ray-tracing technique [7] to numerically calculate the respective propagation loss contributed either by the direct wave or by edge diffraction. The measured and the simulated propagation losses of the first arrived

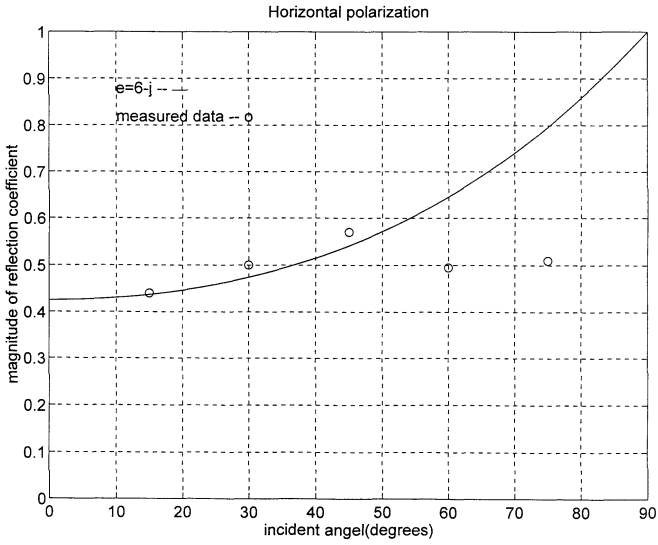


Figure 6. The measured and calculated wall reflection coefficients for various incident angles.

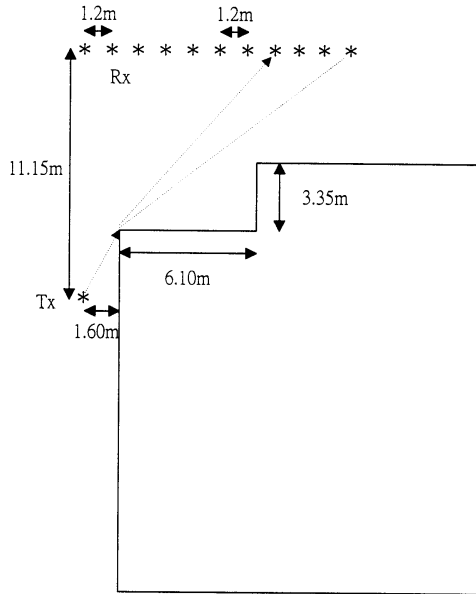


Figure 7. Sketch of the environment for measuring edge diffraction.

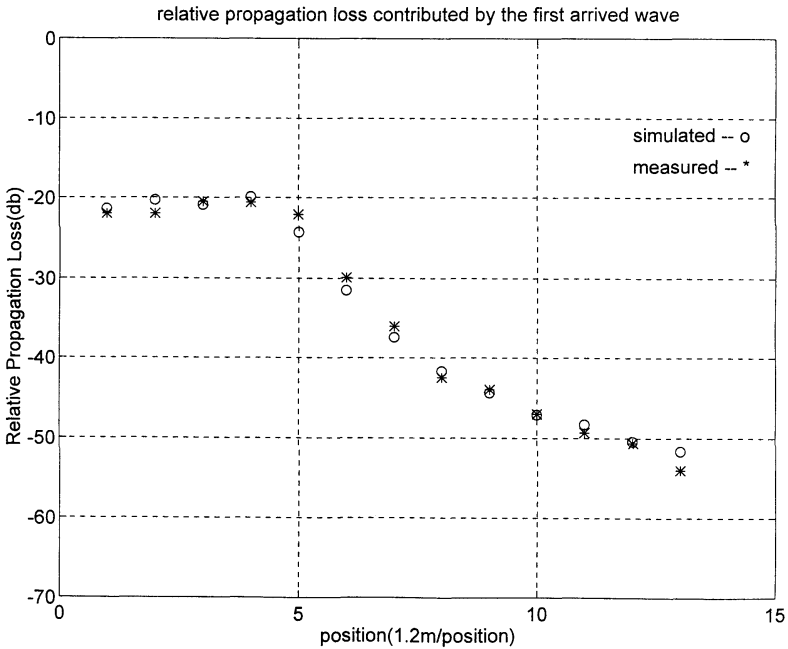


Figure 8. Plot of the measured and simulated propagation loss contributed by the first arrived wave for the geometry of Fig. 7.

wave are shown in Fig. 8. It is seen that after the 5th position, the propagation loss has a sharp decrease. We have also observed that after the 14th position, contribution by double edge diffraction can no longer be identified because it is too small to be distinguished from the random scattering. Most of the deviations between the calculated and the experimental results are within 1dB.

Finally we show the measured and simulated delay profiles of an outdoor radio channel. Fig. 9 show the sketch of the experiment environment. Coordinates of the building corners and the transmitter and receiver positions are also shown in the figure. The transmitting and receiving antennas are both vertically polarized and are at a height of 3m. Fig. 10 (a) and (b) show the measured and simulated delay profiles. In this specific radio channel, the direct path has been obstructed by the corner and the first arrived wave is an edge-diffracted wave. In Fig. 10 (a) we can observe several dominant peaks which are reflected from the walls of surrounding buildings. By examining the layout of Fig. 9 and from the corresponding delay times of the peaks (marked

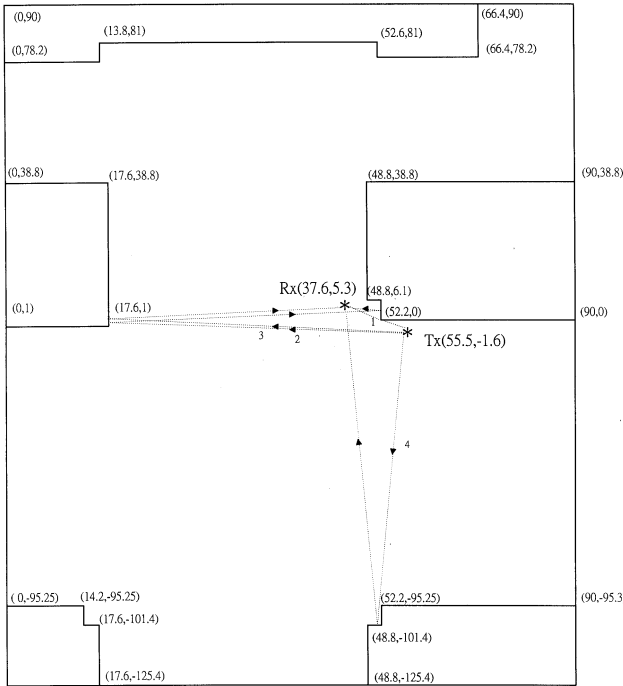


Figure 9. Sketch of the experiment environment and the path traveled by multiple reflections.

by digit numbers in Fig. 10) we can trace the paths of these reflected waves, which are demonstrated in Fig. 9. By comparing Fig. 10(a) and 10(b) we can find some similarities and some differences. The measured one has several peaks not found in the simulated results. This may be due to the scattering not being considered in the simplified simulation input. In the simulated results there are many small peaks caused by edge diffractions and multiple reflections. However, these peaks cannot be identified in the measured delay profile because the amplitudes of these peaks are smaller than the background floor of Fig. 10(a). A dashed line, which corresponds to free space attenuation, is also shown in the figure. The difference between the dashed curve and each peak value represents the edge diffraction coefficient or the reflection coefficient (single reflection) or multiplication of several reflection coefficients (multiple reflections). It is noted that the roughness factor

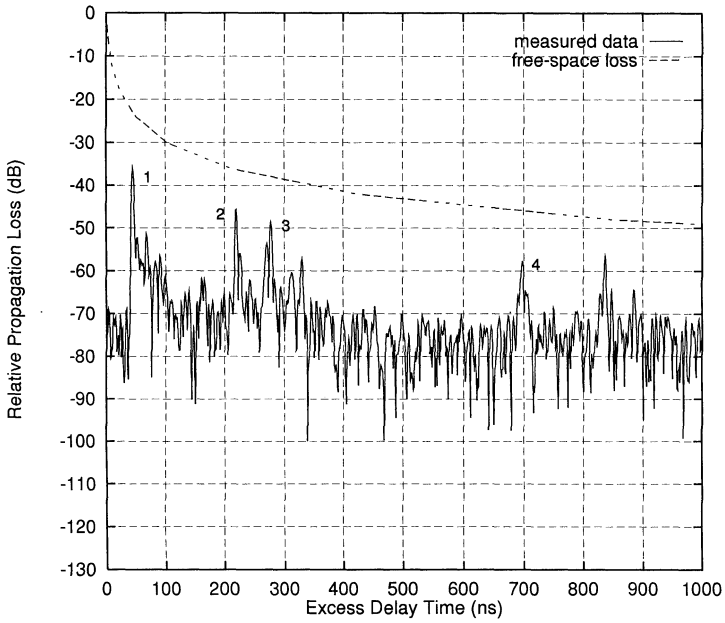


Figure 10.(a) The measured delay profiles.

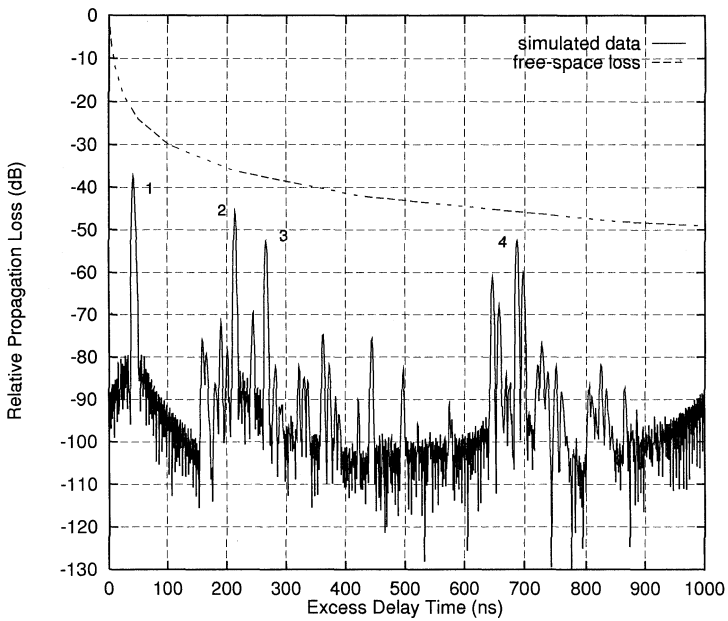


Figure 10.(b) the simulated delay profiles.

of the wall can also be derived from the corresponding difference if the wall dielectric constants are available and its reflection coefficient with smooth surface can be calculated.

6. CONCLUSION

In this paper we have proposed wideband measurement techniques to determine propagation mechanisms. Factors which can affect the accuracy of the measurements are analyzed. Delay profiles can be obtained by applying IFFT on the measured frequency response. To avoid range ambiguity in the delay profile, the frequency response should be finely sampled. Enough zeros should be padded to the measured frequency response before applying IFFT if the peak values sampled in the delay profiles are to be used for representing certain scattering mechanisms such as reflection coefficients or edge diffraction coefficients. In this paper we also propose a calibration procedure so that the ordinate value in the delay profile can represent the propagation loss relative to that at the reference position. We have employed wideband measurements to obtain delay profiles of outdoor radio channels, and from which we can determine wall reflection coefficients and edge diffraction contributions. Measurement results have been compared with simulation results obtained by the ray-tracing technique. Consistency between the experimental and simulation results shows the effectiveness of the proposed methods.

ACKNOWLEDGEMENT

This work is supported by the National Science Council, Republic of China, under the grant number NSC 86-2221-E-002-036.

REFERENCES

1. Cox, D. C., "Delay doppler characteristics of multipath delay spread and average excess delay for 910MHz urban mobile radio paths," *IEEE Trans. on Antennas and Propagation*, Vol. Ap-20, No. 5, 625–635, 1972.
2. Rappaport, T. S., *Wireless Communications, Principle and Practice*, Chap. 3, Prentice Hall PTR, 1996.
3. Pahlavan, K., and A. H. Levesque, *Wireless Information Networks*, Chap. 8, John Wiley & Sons, 1995.

4. Landron, O., M. J. Feuerstein, and T. S. Rappaport, "A comparison of theoretical and empirical reflection coefficients for typical exterior wall surface in a mobile radio environment," *IEEE Trans. on Antennas and Propagation*, Vol. 44, No. 3, 341–351, 1996.
5. Kouyoumjian, R. G., and P. H. Pathak, "A uniform geometrical theory of diffraction for an edge in perfectly conducting surface," *Proc. IEEE*, Vol. 62, 1448–1461, 1974.
6. Ament, W. S., "Toward a theory of reflection by a rough surface," *Proc. IRE*, Vol. 41, No. 1, 142–145, 1953.
7. Jan, S. C., and S. K. Jeng, "Propagation modeling using hybrid SBR, image, and UTD method in urban environment," *Proc. International symposium on Communications*, Taipei, Taiwan, Vol. 2, 1132–1137, Dec. 1995.